Astron. Astrophys. 60, 233—249 (1977)

ASTRONOMY AND ASTROPHYSICS

Aperture Synthesis Observations of Galactic H II Regions

VI. Several Isolated H II Regions

F. P. Israël

Sterenwacht, Huygens Laboratorium, Wassenaarseweg 78, Leiden 2405, The Netherlands*

Received: November 4, 1976; revised March 1, 1977

Summary. Radio maps at λ 21 cm of S 90, S 104, S 125, S 142 and S 184, and at λ 6 cm of S 90, DR 15 and S 228 are presented. Near S 184 and S 104 point sources are found that might be compact H II regions. The nebulae S 125, S 142 and S 184 show very little small-scale structure. They are probably old H II regions in which density inhomogeneities have expanded into more diffuse surroundings. DR 15 and S 228 show small-scale structure, but not with very high contrast. Near DR 15, a large diffuse and totally obscured H II region is present. Both S 90 and S 104 show a shell-like structure. This may be explained by a semi-stationary model in which ionized gas streams away from a neutral cloud through an ionization front.

Key words: radio observations — structure of H II regions — star formation

I. Introduction

This paper presents detailed radio maps of nine galactic H II regions at wavelengths of 6 and 21 cm. The original survey contained two more H II regions: S 206 (NGC 1491) and S 252 (NGC 2175). These are however discussed elsewhere (Deharveng et al., 1976; Felli et al., 1977).

The criteria for selecting these regions were: (i) good optical visibility; (ii) diameter of well-defined brightest parts less than 6′; (iii) known presence of radio emission stronger than 0.5 f.u. and (iv) declination preferably higher than +30°. These criteria were however not strictly adhered to, as is clear from a glance at Table 1.

In that Table, all H II regions are listed which were included in the observed fields. In order to derive physical parameters from the radio observations, the distance of the regions must be known. In Table 2 I list the available radial velocity data. In Column 4 the kinematical distance is given.

Table 1. The observed H II regions

Name	Equatorial coordinates		Galactic coordinates		Optical size (′)
	(1950.0)	(1950.0)	l	b	
(1)	(2)	(3)	(4)	(5)	(6)
S 90	19^h47^m	26°41′	63°.10 + 0°.46		8 × 3
S 104	20 16	36 40	74.83 + 0.62		7 × 7
DR 15	20 31	40 04	79.31 + 0.28		—
S 125 = IC 5146	21 52	47 00	94.43 − 5.58		10 × 10
S 142 = NGC 7380	22 45	57 45	107.04 − 0.97		25 × 20
S 143	22 47	57 21	123.17 − 1.5		4 × 4
S 184 = NGC 281	00 50	56 20	123.31 − 6.28		35 × 30
S 228	05 10	37 20	169.24 − 0.94		2 × 2

For most regions, Georgelin et al. (1973) and Georgelin (1975) list the exciting stars. Their data are summarized in Table 3.

Column 5 gives the distance derived from the stellar distance modulus. As can be readily seen, the distance values in Table 2 and 3 do not agree very well for S 90 and S 142. The discrepancy for S 90 was already noted by Georgelin et al. (1973). The radial velocity derived by Lozinskaya and Esipov (1974) for S 104 is surprisingly high compared with the other two values. The distances I adopt are included in Table 7, Column 9. Some of them will be discussed in more detail in Section III.

Previous (single dish) radio observations of the regions are summarized in Table 4. With the exception of S 104 (see Section III.3) all appear to have optically thin, thermal spectra.

The observed H II regions have one common characteristic. They are all larger than 1 pc. Together with their good optical visibility (DR 15 excepted) this indicates that they are evolved H II regions, probably older than 10^5 years. Thus they present an opportunity to study the structure of H II regions in a later stage than the compact H II regions.

* *Present address:* Owens Valley Radio Observatory California Institute of Technology, Pasadena, CA 91125, USA

Table 2. Radial velocities

Name (1)	Line (2)	V_{LSR} (km s^{-1}) (3)	D_{kin} (kpc) (4)	Ref. (5)
S 90	H 109α	+15.3±2.8	1.4	Reifenstein et al. (1970)
	Hα	+22.5	2.3	Georgelin et al. (1973)
	CO	+22.2	2.3	Blair et al. (1975)
S 104	H 109α	no detection	2.3	Reifenstein et al. (1970)
	H 109α	0±4	–	Dickel and Milne (1972)
	Hα	−0.4	5.3	Georgelin et al. (1973)
	Hα	18±3	3	Lozinskaya and Esipov (1974)
G 74.9+1.2	H 109α	no detection	–	Reifenstein et al. (1970)
DR 15	H 109α	− 1.6	4	Reifenstein et al. (1970)
S 125	HI	+ 6.9	3.0	Riegel (1967)
	Hα	+ 4.8	–	Georgelin et al. (1973)
	Hα	+ 2.1±6.0	0.9	Miller (1968)
	CO	+ 7.6	–	Milman et al. (1975)
S 142	Hα	−35.4	3.1	Courtès et al. (1966)
	Hα	−45.3±1.2	5.4	Miller (1968)
	Hα	−35.8	3.2	Georgelin et al. (1973)
S 184	Hα	−27.8	2.0	Courtès et al. (1966)
	HI	−30	2.2	Riegel (1967)
	Hα	−31.2	2.3	Miller (1968)
	Hα	−27.8	2.0	Georgelin et al. (1973)
S 228	Hα	− 9.4	2.6	Georgelin and Georgelin (1970)
	CO	− 8.3	–	Dickinson et al. (1974)

Table 3. Exciting stars

Name (1)	Star (2)	Spectral Type (3)	App. Vis. Mag. V (4)	D_{star} (kpc) (5)
S 90	LS II 26°6	O9.5III	11.4	4.0
S 104	—	O5	12.2	4.4
S 125[a]	BD 46°3474	B_1 V?	9.6	1.0
S 142	HD 215835	O6n	8.6	2.8
S 143	LS III 57°93	O9.5V	10.8	4.9
S184	HD 5005	O6	7.7	1.7

[a] Walker (1959)

II. Observations and Reduction

All observations were made with the Westerbork Synthesis Radio Telescope. The telescope has been described in detail by Baars and Hooghoudt (1974). The λ 21 cm continuum receiver system was described by Casse and Muller (1974). Details relevant to the observations are given in Tables 5 and 6.

I used the standard calibration and reduction procedures (Högbom and Brouw, 1974; Van Someren Greve, 1974). The results on the observed HII regions are given in Table 7, while Table 8 lists other sources found in the observed field.

The following comments are in order.

i) In all maps, interferometer spacings shorter than 36 m are missing. As a consequence, extended structure is inadequately observed in the case of this effect is serious for S 142 and S 184. (See however also Point iii.)

ii) The lack of a zerospacing implies a shift of the zerolevel near the source. In all cases except those of S 142 and S 184 at λ 21 cm and S 90 at λ 6 cm the effect on the maps is only slight as can be verified with cross-cuts. (See also Point iii.)

iii) In order to separate actual source structure from the instrumental effects mentioned in Points i) and ii), the clean procedure (Högbom, 1974; Harten, 1976) was used on the λ 21 cm map of S 184 and the λ 6 cm map of S 90. After cleaning, the extracted delta functions were convolved with the center of the antennapattern (i.e. the the synthesized beam without sidelobes and grating rings) and restored onto the residual maps. This has the effect of eliminating the zerolevel depression and restoring into the map the actual flux densities for all structure inside the first grating ring (which has a dimension of 20×20 cosec δ at λ 21 cm and 6×6 cosec δ at λ 6 cm).

iv) Flux densities of sources discussed in the text were all derived by planimetering the contourmaps; they are corrected for changes in the primary beam sensitivity over the field. At λ 21 cm, the primary beam can be described roughly as a Gaussian of the form $F_1(\%) = 100 \exp(-7.3\ R^2)$ where R is the distance to beam centers in degrees. The estimated accuracy of the flux densities determined in this way is 15%. The (Gaussian) angular sizes were also determined from the contourmaps and corrected for finite beamwidth.

The positions and flux densities of the sources listed in Table 8 were determined from the maps by eye estimates. The sources marked with an asterisk were found by the standard source find procedure. The quoted flux densities are peak values. Since most of the

Table 4. Previous radio observations

Name	Author's designation	Frequency (MHz)	HPBW (′)	Flux-density (f.u.)	Ref.
(1)	(2)	(3)	(4)	(5)	(6)
S 90	T 26	318	16.2	4.6 ±0.5	Terzian (1970)
	BG 1947+26	408	3×10	4.8	Fanti et al. (1974)
	TP 69	606	9	4.4 ±1.1	Terzian and Pankonin (1972)
	S 90	610	17.5	5.2 ±1.9	Wendker (1968)
	S 90	1400	21	8.7 ±1.8	Wendker (1971)
	S 90	1400	10	6.2 ±2	Felli and Churchwell (1973)
	PKS 1947+26.6	1410	13.9	5.4 ±0.4	Shimmins and Day (1968)
	DA 492	1420	36	20	Galt and Kennedy (1968)
	CTD 116	1421	33	5.2 ±1.3	Kellerman and Read (1965)
	G63.2+0.5	2695	10	7 ±2	Altenhoff et al. (1970)
	S 90	2725	5.4	5.5 ±0.3	Willis (unpublished)
	G 63.2+0.4	5000	6.5	4.8 ±1.4	Reifenstein et al. (1970)
S 104	T 34	318	16.2	5.0 ±2.0	Terzian (1970)
	BG 2015+36	408	3×10	5.0	Fanti et al. (1974)
	TP 78	606	9	14.2 ±3.6	Terzian and Pankonin (1972)
	S 104	1400	10	(8)	Felli and Churchwell (1973)
	G 74.8+0.7	2695	10	7 ±2	Altenhoff et al. (1970)
	G 74.8+0.6	4995	6	4.6	Reifenstein et al. (1970)
DR 15		2695	6.5	7.5 ±1.1	Reifenstein et al. (1970)
		2695	11	34.3	Wendker (1970)
		5000	10.8	15.6	Downes and Rinehart (1966)
		7875	4.4	1.6 ±0.6	Johnson (1974)
		15500	2.2	1.5	
S 125	CTA 97	960	48	4.5	Harris and Roberts (1960)
	S 125	1400	10	2.4 ±0.4	Felli and Churchwell (1973)
	DA 567	1420	36	2.2	Galt and Kennedy (1968)
	IC 5146	2695	5.2	2.0 ±0.3	Terzian et al. (1973)
S 142	S 142	1400	10	12 ±2	Felli and Churchwell (1973)
	NGC 7380	2695	11	17 ±1.7	Gebel (1968)
	NGC 7380	4995	6.54	15 ±1.5	Gebel (1968)
S 143	S 143	4850	15×7	< 0.1	Kazès et al. (1975)
S 184		178	20	13.5 ±2	Caswell (1968)
	CTA 6	960	48	15.6 ±1.8	Harris and Roberts (1960)
	CTB 7	960	48	16	Wilson and Bolton (1960)
	S 184	1400	10	19.7 ±3	Churchwell and Walmsley (1973)
	NGC 281	1400	—	15	Osterbrock and Stockhausen (1961)
	DWO 049	1417	37	17.2 ±0.3	Davis (1967)
	DA 025	1420	36	15.4 ±1.5	Galt and Kennedy (1968)
	S 184	2695	18.2	12 ±2.5	Churchwell and Walmsley (1973)
	NGC 281	2695	11	22 ±2.2	Gebel (1968)
	NGC 281	3200	9	22 ±2	Caswell (1968)
	NGC 281	3200	38	22 ±7	RaghavaRao et al. (1965)
	NGC 281	4995	6.4	18 ±1.8	Gebel (1968)
S 228	T 7	318	16.2	1.6 ±0.3	Terzian (1970)
	TP 18	606	9	1.2 ±0.5	Terzian and Pankonin (1972)
	S 228	1400	10	3.4 ±0.5	Churchwell and Walmsley (1973)
	S 228	1416	4×22	1.02	Kazès et al. (1975)
	S 228	2695	18.2	1.8 ±0.6	Churchwell and Walmsley (1973)
	S 228	4890	1.5×7	1.14	Kazès et al. (1975)
	S 228	15500	2.2	0.60±0.42	Johnson (1974)

Table 5. WSRT Parameters

Frequency (MHz)	1415	4995
Wavelength (cm)	21.2	6.0
HPBW Primary Beam (′)	37.6	12
HPBW Synthesized Beam (″)	24.6×24.6 cosec δ	7.2×7.2 cosec δ
R.m.s. Noise per 1×12 h (m.f.u. per beam)	1.2	13
HPW of a gaussian source of amplitude 0.5 at 36 m spacing (′)	9×9 cosec δ	2.5×2.5 cosec δ

Table 6. Observations log

Field	Date	Duration	Fieldcenter	Range of interferometer spacings (m)	Increment (m)
(1)	(2)	(3)	(4)	(5)	(6)
λ 21 cm	Observations				
S 90	July 1971	1 × 12 h	$19^h47^m00^s$ 26°52 48	36–1404	72
G 74.9+1.2	Dec. 1973	1 × 12 h	20 14 00 37 06 00	36–1404	72
S 104	July 1971	1 × 12 h	20 15 00 36 45 00	36–1404	72
S 125	May/June 1974	2 × 12 h	21 54 24 47 03 29	36–1440	36
S 142	Sept. 1971	1 × 12 h	22 45 18 57 46 34	36–1404	72
S 184	Dec. 1973	1 × 12 h	00 50 06 56 21 00	36–1404	72
λ 6 cm	Observations				
S 90	March 1974	1 × 12 h	19 47 12 26 45 00	36–1404	72
DR 15	July 1973 Aug. 1973 Oct. 1973	1 × 12 h	20 30 36 40 04 12	36–1404	72
S 228	Aug. 1973	1 × 12 h	05 10 00 37 28 24	36–1404	72

sources show little or no beam broadening, the error introduced by this is small.

III. Discussion of Individual Regions

1) Physical Parameters

I used the observed parameters given in Table 7 and equations derived by Mezger and Henderson (1967) in order to calculate the model physical parameters given in Table 9.

In this calculation, it was assumed that the HII regions have the shape of a cylinder whose depth equals its diameter, that they consist of homogeneously distributed hydrogen, that they radiate at 10^4 K and that they are optically thin. Thus the r.m.s. electron density n_e is a lower limit to the actual electron density, and the mass M is an upper limit to the actual mass. The emission measure E.M. is independent of distance, while the excitation parameter u is independent of the assumed model.

A discussion of the individual HII regions now follows.

2) S 90 (G 63.17+0.46)

In a dusty area between the constellations Hercules and Lyra, a small curiously shaped nebula is seen. It is prominent on the red Palomar Sky Survey print, but barely visible on the blue one. It has the shape of a semi-circular shell, with weak diffuse emission plumes at the extremes (Fig. 1). Its radial velocity indicates a distance of either 2.3 or 6.8 kpc because of the distance ambiguity of objects inside the solar circle. One possible exciting star (Table 3) is of spectral type O9.5III and appears to be at a distance of 4 kpc. It is located far from the brightness center of the nebula (Fig. 2). In the λ 21 cm map (Fig. 2) a flux-density of 4.8 f.u. is observed, in the λ 6 cm map (Fig. 3) a flux density of 4.6 f.u. This agrees well with previously determined values (Table 4) so that the maps show essentially all radio emission of S 90.

For the near distance of 2.3 kpc, an excitation parameter of 42 pc cm^{-2} follows. An O9.5III star should have an excitation parameter of 47 pc cm^{-2} (Panagia, 1973). However, Chopinet and Lortet-Zuckermann (1975) expect another exciting star of type O7 to be present in S 90 on the basis of the observed nebular [OIII]/Hβ ratio of two. In the following I adopt $D=3.5$ kpc, agreeing that at least one more exciting star must be present.

Both radiomaps resemble the optical picture to a certain extent. The ridge-like structure is clearly present in both radiomaps; the contrast between the ridge and the rest of the nebula is in the optical however much larger than in the radio (cf. Figs. 1 and 4). Apparently, dust obscures most of the diffuse emission in S 90. The ridge has a flux density of 295 m.f.u. and a size of about 0.5 (corresponding to a linear size of 0.5 pc at a distance of 3.5 kpc). It has an r.m.s. electron density of 485 cm^{-3} as compared with an r.m.s. electron density of 110 cm^{-3}

Table 7. Observed parameters

Name	Right ascension (1950.0)	Declination (1950.0)	Gal. long l	Gal. lat. b	Flux-density S_{1415} (f.u.)	Flux-density S_{4995} (f.u.)	Equivalent gaussian angular diameter (′)	Adopted distance (kpc)
S 90	$19^h47^m08^s$	26°44′00″	63.176	+0.46	5.8 ±0.7	5.0 ±1.0	3.4	2.3
G 74.9+1.2[a]	20 14	37 04	74.94	+1.18	8.4 ±1.3	–	7	–
S 104	20 15 48	36 35 45	75.11	+0.86	5.0 ±0.7	–	5.7	5.0
DR 15A	20 30 40.3	40 05 48	79.297	+0.281	–	0.07±0.01	0.08	4.0
B	20 30 39.6	40 06 55	79.311	+0.294	–	0.15±0.02	0.4× 0.3	
C	20 30 41.7	40 05 56	79.301	+0.279	–	0.11±0.02	0.2× 0.5	
D	20 30 42.6	40 06 04	79.305	+0.278	–			
E	20 30 43.8	40 06 16	79.310	+0.277	–	{0.64±0.10}	{0.65× 0.8}	
F	20 30 40.2	40 06 13	79.302	+0.285	–			
Inner envelope	20 30 42	40 06 15	79.31	+0.28	–	3.31±0.4	1.2 × 2.4	
Outer envelope	20 30 42	40 06 15	79.31	+0.28	–	1.5 ±0.2	3.7 × 1.9	
G 79.2+0.4	20 30 12	40 05 00	79.2	+0.4	–	1.7 ±0.2	2.7	4.0
S 125	21 51 30	47 03 00	94.40	−5.48	1.6 ±0.2	–	5.1 × 5.4	1.0
S 142	22 45 52	57 49 30	107.18	−0.95	12.1 ±2.0	–	13.2 ×10.0	4.0
S 143	22 47	57 21	107.10	−1.45	≤0.3	–	(3.3 × 3.3)	5.0
S 184 total	00 50	56 18	123.16	−6.5	6.2 ±0.5	–	7.8 × 6.6	2.0
A	00 49 25	56 18 10			0.25±0.05	–	3.0 × 1.1	
B	00 50 20	56 19 00			0.15±0.03	–	1.1 × 3.0	
S 228 Core	05 10 02	37 23 30	169.192	−0.903	–	0.6 ±0.1	1.4 × 1.6	2.6
Envelope	05 10 00	37 23 15	169.19	−0.90	–	0.7 ±0.1	2.9	

[a] Probably Supernova Remnant; see Duin et al. (1975)

for the nebula as a whole. The peak emission measure is about 10^5 pc cm^{-6}, more than twice the peak emission measure of S 90 as a whole. Both the linear diameter of 4.7 pc and the r.m.s. electron density of 110 cm^{-3} qualify S 90 as an HII region evolved beyond the compact stage. The peculiar optical and radio structure may indicate strong dynamical interactions between the exciting star and the surrounding medium. More likely, however, the morophology is the consequence of a geometry like that of S 206 (Deharveng et al., 1976) where dense ionization front appears to be eating its way into a neutral cloud. Indeed, Blair et al. (1975) found an intense and large (size more than 8′) CO cloud at the position and velocity of S 90. The radial velocity of the CO cloud is the same as the Hα radial velocity found by Georgelin et al. (1973) but differs considerably from the H 109 α velocity found by Reifenstein et al. (1970) which is lower by 7 km s^{-1}. The Hα velocity reflects the velocity of the bright ridge, while the H 109 α velocity is almost completely determined by the diffuse gas that is visible in the radiomaps. This diffuse gas is therefore streaming towards us with respect to the bright ridge. In order to understand the precise nature of S 90, a detailed optical study of the velocity field and the extinction across the nebula is necessary.

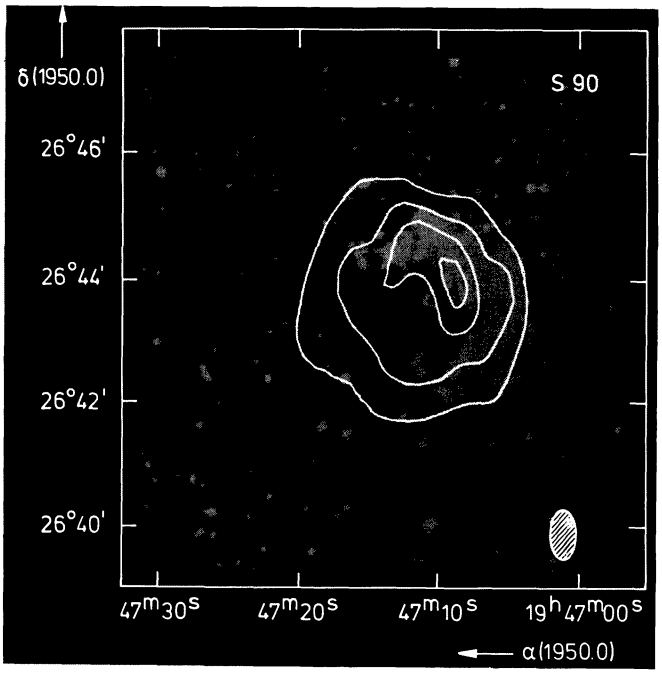

Fig. 1. S 90. Radio contours at λ 21 cm are superimposed on the red Palomar Sky Survey print. The contours have values of 50, 100, 150 and 200 m.f.u. per synthesized beam area. In this, and in the following figures, a shaded ellipse indicates the synthesized beam

3) S 104 (G 74.83+0.62)

In the very confused Cygnus area, the nebula S 104 is found. On the red Palomar Sky Survey print it shows a shell-like structure. The south eastern part of the shell is much brighter than the western part. Because of its shape and the apparent absence of H 109 α recombination line emission (Reifenstein et al., 1969) it was for some time regarded as a supernova remnant (Milne, 1970;

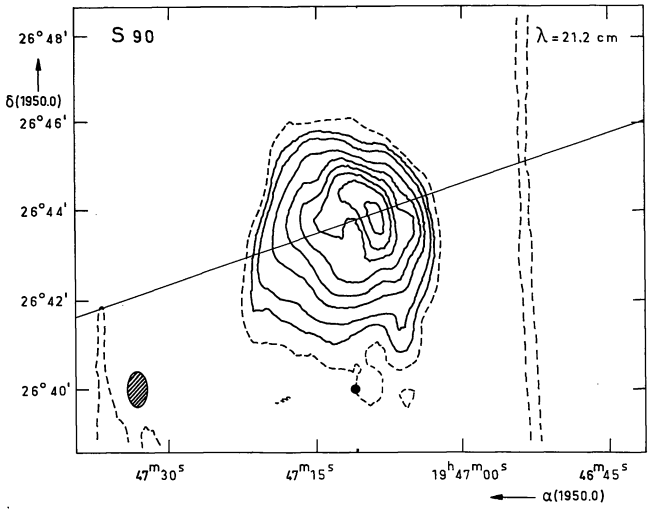

Fig. 2. S 90. Radio map at λ 21 cm, showing contours of 12.5, 25, 37.5, 62.5, 87.5, 112.5, 137.5, 162.5 and 200 m.f.u. per synthesized beam area. The supposed exciting stars LS II 26°6 is marked by a dot

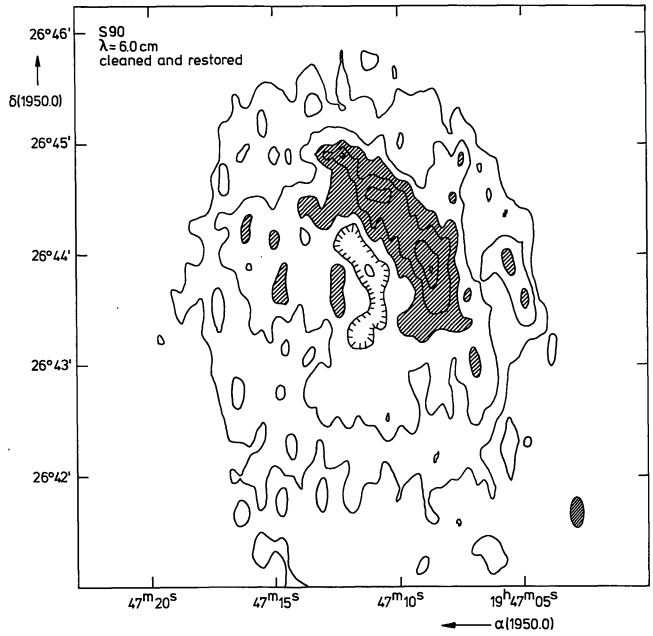

Fig. 3. S 90. Radio map at λ 6 cm showing contours of 5, 10, 15, 20, 25 and 30 m.f.u. per synthesized beam area. The ridge is shaded

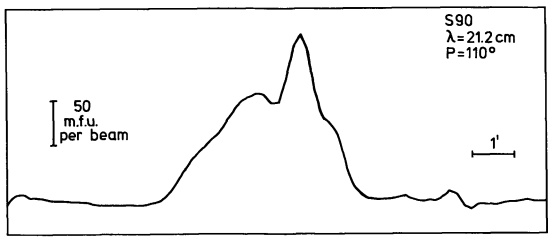

Fig. 4. Cross-cut through S 90 at λ 21 cm. The direction of the cut is indicated in Figure 2

Table 8. Other sources

Number	Field	Right ascention (1950.0)	Declination (1950.0)	Flux-density S_{1415} (f.u.)
1*	S 90	$19^h45^m22^s.8$	26°46'19"	0.670
2		19 45 35	26 28 30	0.060
3		19 45 48	26 55 30	0.017
4*		19 46 56.9	27 08 53	0.032
5*		19 48 45.4	26 58 52	0.284
6	S 104	20 13 12	36 16 48	0.390
7*		20 13 37.0	37 01 45	1.155
8[a]		20 13 49	36 31 30	0.050
9		20 14 04	36 50 14	0.050
10*		20 14 35.2	36 45 41	0.056
11*		20 14 55.3	36 22 13	0.025
12[a]		20 15 53	36 41 21	0.035
13[a]		20 16 03	36 36 17	0.085
14		20 16 31	36 57 54	0.015
15		20 16 40	36 52 12	0.025
16*	S 125	21 48 15.9	47 01 11	0.042
17		21 49 01	47 16 50	0.017
18*		21 49 46.6	47 25 14	0.032
19*		21 50 17.8	47 12 29	0.019
20		21 50 24	47 07 30	0.006
21*		21 50 25.7	46 46 53	0.023
22		21 50 27	47 12 50	0.018
23*		21 50 48.7	47 03 27	0.006
24*		21 50 59.6	47 19 01	0.007
25*		21 51 39.8	47 07 02	0.062
26*		21 51 43.2	47 12 40	0.038
27		21 51 50.2	47 08 46	0.009
28		21 52 01.6	47 10 25	0.048
29*	S 142	22 43 13.2	58 09 48	0.144
30*		22 44 12.1	57 54 03	0.024
31*		22 44 18.4	58 06 52	0.034
32*		22 44 35.8	57 26 46	0.248
33*		22 44 46.2	57 47 19	0.035
34*		22 48 25.5	57 50 28	0.110
35*	S 184	00 49 20.6	56 33 44	0.019
36*		00 49 26.0	56 32 29	0.047
37*[b]		00 49 46.8	56 14 33	0.104
38*		00 49 57.5	56 47 16	0.089
39		00 49 59	56 48 00	0.075
40*		00 51 37.8	56 23 50	0.023
41*		00 51 48.6	56 31 51	0.056
42*		00 51 53.7	56 30 37	0.080
43*		00 51 54.7	56 34 17	0.040
44*		00 53 46.3	56 25 14	0.172

[a] See text, Section III.4
[b] See text, Section III.9

Downes, 1971). The radio observations of the source, especially the difference between the high frequency points and the 606 MHz point due to Pankonin and Terzian (1972) seemed to confirm the non-thermal nature of S 104. However, Dickel and Milne (1972) subsequently succeeded in detecting weak H 109 α line emission, while Georgelin et al. (1973) and Lozinskaya and Esipov (1974) observed Hα emission characteristic of an HII region. Both Lozinskaya and Esipov (1976) and Johnson (1975) noted that the optical spectrum of S 104 is characteristic of a normal HII region. Yet

Table 9. Derived parameters

Name	Linear diameter d(pc)	R.m.s. Electron density n_e (cm^{-3})	Emission measure E.M. (10^4 pc cm^{-6})	Mass $M(M_0)$	Excitation parameter u(pc cm^{-2})	Excitation expected by star of type earlier than
(1)	(2)	(3)	(4)	(5)	(6)	(7)
S 90	4.1	110	5.3	155	56	O 7
S 104	9.9	41	1.6	780	68	O 6
DR 15A	0.1	6885	133	0.09	15	B 0
B	0.5	505	12.4	1.1	18	B 0
C	0.5	450	10.0	1.0	17	B 0
D						
E	1.0	360	13.2	7.2	29	O 9.5
F						
Inner envelope	2.6	200	12.0	64	50	O 7.5
Outer envelope	3.7	69	2.2	82	40 total 64	O 6
G 79.2+0.4	3.8	70	2.2	74	39	O 8
S 125	1.8	57	0.6	7	16	B 0
S 142	16	25	1.0	1985	78	O 6
S 143	5.7	$\leqslant$ 23	$\leqslant$ 0.3	$\leqslant$ 84	$\leqslant$26	$\leqslant$O 9.5
S 184 total	5.0	50	1.3	125	39	O 8
A	1.3	81	0.8	3.1	14	B 0.5
B	1.5	62	0.5	2.4	11	B 0.5
S 228 Core	1.4	154	3.3	7.5	23	B 0
Envelope	2.6	62	1.0	22	24 total 29	B 0 (O 9.5)

Lozinskaya and Esipov (1974) suggested that S 104 might be a type I supernova remnant in a relatively dense neutral medium; they based this notion mainly on the seemingly non-thermal radio spectrum.

Table 4 shows the 606 MHz point to be anomalously high [possibly due to confusion with the nearby source G 74.9+1.2, which indeed has a non-thermal spectrum, cf. Duin et al. (1975)] while the WSRT 1415 MHz point agrees reasonably well with the other observations of Table 4 on the assumption of an optically thin thermal spectrum. Thus there is little doubt that S 104 is a normal HII region.

The optical and radio pictures (Fig. 5 and 6) look identical, but the optical brightness asymmetry is not reproduced in the radiomap, indicating that the western part of S 104 suffers a larger extinction than the eastern part. Lozinskaya and Esipov (1974) estimate the Hα surface brightness $S(\mathrm{H}\alpha)=4\ 10^{-5}$ erg cm^{-2} s^{-1} sterad^{-1}. This value must be taken with considerable caution, since it is not a direct measurement, but only an estimate of the Hα surface brightness. Taken at face value, it would predict a radio flux density of $S_{1415}=0.15$ f.u., whereas the observed value is 5 f.u. The difference implies an extinction at the wavelength of Hα of $3^{\mathrm{m}}9$. Assuming a standard reddening law (Whitford, 1958) this in turn leads to $A_V=5^{\mathrm{m}}0$. That is somewhat higher than $A_v=4^{\mathrm{m}}7$ Lozinskaya and Esipov themselves quote, but in view of the uncertainties the agreement is close.

The exciting star is not obvious on Palomar Sky Survey prints. Georgelin (1975) finds S 104 to be excited by an O5 star with a true distance modulus of $13^{\mathrm{m}}2$ ($D=4.5$ kpc). Sharpless, as quoted by Johnson (1975) also assigns a spectral type of O5 to the exciting star, but gives a distance modulus of $13^{\mathrm{m}}6$ ($D=5.2$ kpc). Taking $M_V=-5^{\mathrm{m}}8$ for an O5 star (Panagia, 1973), one finds again $A_V=4^{\mathrm{m}}7-5^{\mathrm{m}}1$.

Thus the extinction of S 104 appears to be well-determined. In the following I will adopt $D=5$ kpc.

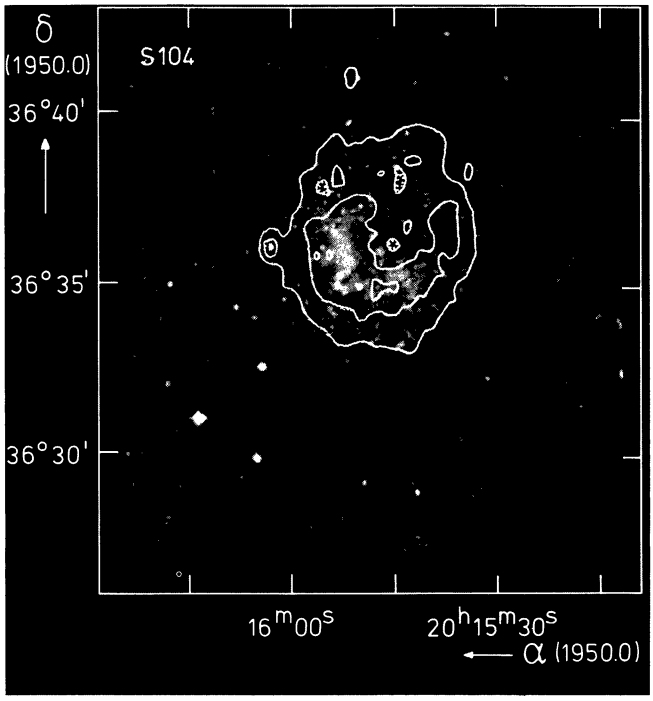

Fig. 5. S 104. Radio contours at λ 21 cm are superimposed on the red Palomar Sky Survey print. The contour values are 12.5, 25. 37.5 and 50 m.f.u. per synthesized beam area

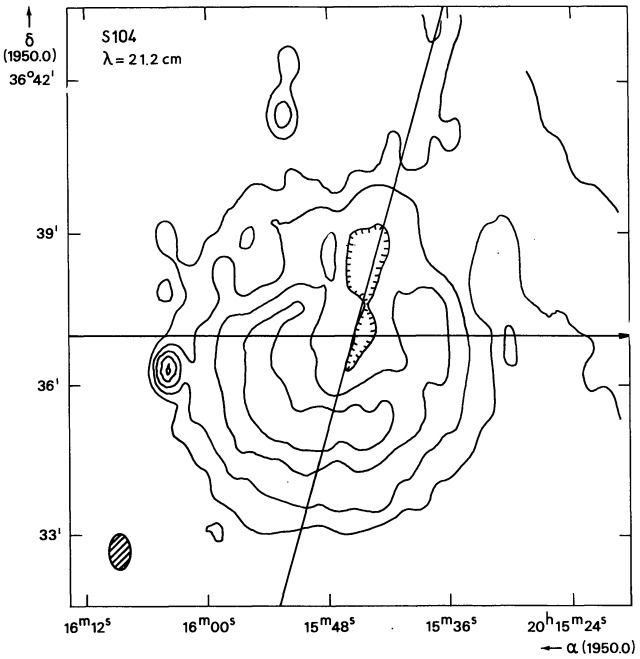

Fig. 6. S 104. Radio map at λ 21 cm showing contours of 10, 20, 30, 40 and 60 m.f.u. per synthesized beam area

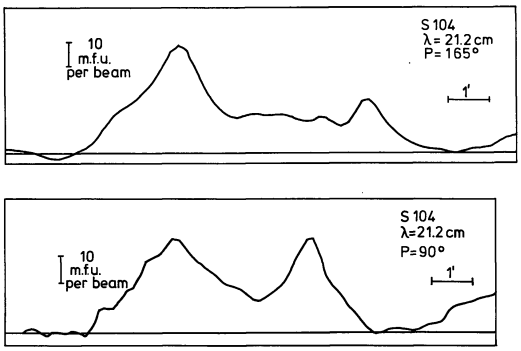

Fig. 7. Cross-cuts through S 104 at λ 21 cm. The direction of the cuts is indicated in Figure 6

The excitation parameter of S 104 is then 68 pc cm^{-2} corresponding only to an O6.5 star (Panagia, 1973). The nebula is therefore probably mass-limited, in accordance with its optical appearance. If one tries to allow for the shell-like structure (see also Fig. 7) by treating the nebula as a homogeneous sphere with outer diameter $\theta = 6'.8$ containing a spherical cavity with diameter $\theta = 2'.7$, this leads to slightly different physical parameters: an r.m.s. electron density of 40 cm^{-3}, a mass of $800 M_\odot$ and a peak emission of 1.6 10^4 pc cm^{-6}. The excitation parameter remains unchanged.

The low electron density and the large diameter of S 104 imply that it is a rather old HII region. A weak CO cloud is found to be associated with S 104 (Cong, private communication).

4) Small-diameter Sources Near S 104

At the eastern edge of S 104 one finds a point source (No. 13 in Table 8) with $S_{1415} = 85$ m.f.u. As it appears unresolved, its angular diameter is less than 15″. The nature of this source is unknown. No optical counterpart is visible, so that it is probably not a bright rim or externally ionized globule. Its position exactly at the edge of S 104 suggests the possibility that it is an obscured compact HII region. In that case its r.m.s. electron density must exceed 6 10^2 cm^{-3}, its emission measure must be larger than 1.5 10^5 pc cm^{-6}, while its excitation parameter is 17 pc cm^{-2}. Its linear diameter should be less than 0.4 pc. The object may be optically thick, in which case the excitation parameter is also a lower limit.

In the field of S 104, two other small radio sources appear coincident with stellar, perhaps slightly fuzzy images on the red Palomar Sky Survey print. These are sources Nos. 8 and 12 from Table 8. One must bear in mind however, that the star field around S 104 is very crowded, so that the identifications are only tentative. Source No. 8 is well resolved with a corrected (Gaussian) diameter of 45″ (Fig. 8). If it is at the distance of 5 kpc as S 104, this indicates a linear (cylindrical) size of 1.3 pc. The source has a flux density of 80 m.f.u. and it is definitely red on the Palomar Sky Survey prints. If it is an HII region, it has an r.m.s. electron density of 110 cm^{-3}, a mass of 4.7 $M_\odot$ and an emission measure of 1.5 10^4 pc cm^{-6}, so that it hardly qualifies as a compact HII region. It could be excited by a B0 star.

The second object, source No. 12 appears unresolved. It is quite close to S 104, less than 1.′5 from its northern edge. It is visible in Figure 6. The flux density of the object is only 35 m.f.u. If it is an HII region, it might be a compact HII region, because its r.m.s. electron density must be larger than 370 cm^{-3}, its linear diameter must be less than 0.4 pc, and its peak emission measure must exceed 6 10^4 pc cm^{-6}.

5) DR 15 (G79.31+0.28)

The source DR 15 (Downes and Rinehart, 1966) is located in the heavily obscured Cygnus X region; it has a weak optical counterpart (Wendker, 1970). DR 15 was found to be an infrared source with an infrared luminosity of $L_{40-350} = 4\ 10^5\ L_\odot$, indicative of excitation by one O6 star (Emerson et al., 1973). In the λ 6 cm map (Figs. 9 and 10) I detect $S_{4995} = 5.8$ f.u., which taken together with an assumed distance $D = 4$ kpc indicates excitation by an O7 star. An extended diffuse emission region with $S_{4995} \approx 1.7$ f.u. is found a few arc min to the west of DR 15.

The sum of these flux densities agrees well with Reifenstein's (1970) value $S_{2695} = 7.5$ f.u. observed with a HPBW of 6.′5. The high flux densities found by Wendker

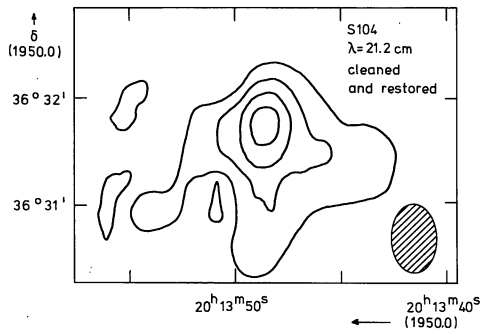

Fig. 8. Source No. 8 at λ 21 cm. Contour values are 5, 10, 15 and 20 m.f.u. per synthesized beam area. The lowest contour might not be significant

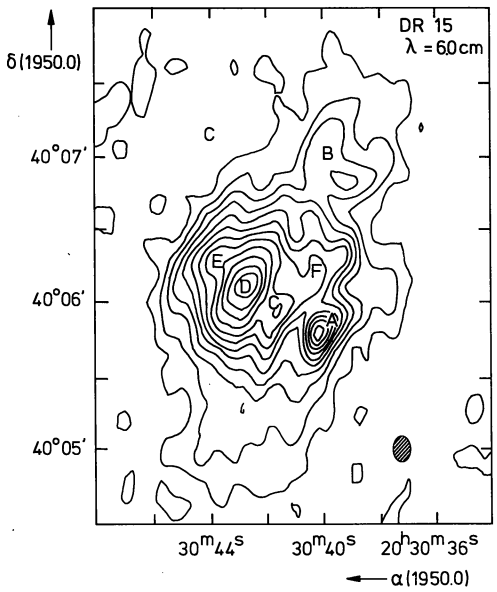

Fig. 9. DR 15. Radio map at λ 6 cm showing contours of 5, 10, 15, 20, 25, 30, 35, 40, 45, 50 and 60 m.f.u. per synthesized beam area

(1970) and Downes and Rinehart (1966) are clearly due to confusion and local zerolevel problems (cf. their contour maps).

The structure of DR 15 is complicated (Fig. 9). The source shows the characteristics of a cluster of dense objects embedded in a common envelope. Component A seems to be a true compact HII region with $n_e = 6885$ cm^{-3} and a linear size $d = 0.1$ pc. The other components have lower r.m.s. electron densities and somewhat larger densities.

The DR 15 complex is reminiscent of the nearby DR 21 complex (Harris, 1973) and the W3OH complex (Harten, 1976). It can be explained in terms of a cluster of OB stars in an early stage of development. The low excitation parameters of the small components derived from the radio emission may be misleading: due to a combination of optical depth effects in both the gas and the dust the actual spectral type of the exciting star may well be underestimated (De Jong et al., 1975). In this respect one notes that the far infrared luminosity $L_{40-350} = 4\ 10^5\ L_\odot$ observed by Emerson et al. (1973) indicates excitation by one O6 star or alternatively 6 O8 stars, while only 2 O8 stars are needed to provide the observed radio luminosity. At present, it is impossible to tell whether the difference is explained by optical depth effects or confusion effects. Probably a combination of both applies since the far-infrared source has a size of 5′ (Emerson et al., 1973) while the mean size of the radio source is only 2′.8. The presence of a second diffuse emission region nearby complicates the picture. One notes that the OH1667 absorption line observations in the direction of DR 15 show weak absorption at $V_{LSR} = +1.4$ km s^{-1} (Paschenko, 1974). DR 15 appears to lie near the northeastern edge of a normal interstellar cloud with a size of 80 pc and a density of one hydrogen atom per cm^{-3} (Paschenko, 1974). It is however doubtful whether DR 15 is actually associated with this cloud.

6) G79.2+0.4

The object near DR 15 is presumably an HII region. Its apparent physical parameters (r.m.s. electron density of 70 cm^{-3}, size of 3.8 pc and excitation parameter of 39 pc cm^{-2}) indicate it to be a rather normal emission nebula of the classical kind. It does not contain compact HII regions, it is probably well evolved, and it has probably nothing to do with DR 15.

7) S 125 (=IC 5146; G94.4−5.6)

Optical photographs show S 125 as a bright nebula, situated in the center of a dense dust cloud, which in turn is only part of a very striking, elongated dust cloud that stretches westward for more than two degrees. Well-exposed photographs show irregular dark spots in front of the nebula. S 125 is very bright on both the red and the blue Palomar Sky Survey prints (Fig. 11). Herbig (1959) found a strong optical continuum, indicating that the nebula contains also large amounts of reflecting dust. The nebula S 125 evelopes the star cluster IC 5146, which was studied in detail by Walker (1959). He concluded that the cluster is about 3 10^6 years old and that it is at a distance of 1 kpc. The exciting star of the nebula appears to be BD+46°3474 which is classified as a BIV star. It has an apparent magnitude $V = 9^m.6$. Walker (1959) derived a corrected apparent magnitude $V_0 = 6^m.5$. Together with a distance modulus of $10^m.1$ this yields an absolute visual magnitude $M_V = -3^m.6$. According to the calibration by Walborn (1972) and to data discussed by Panagia (1973) this indicates a star of spectral type B0V−B0.5V rather than B1V.

The λ 21 cm radiomap (Fig. 12) shows a symmetrical, rather featureless nebula. The overall emission measure is low: only 6.2 10^3 pc cm^{-6}.

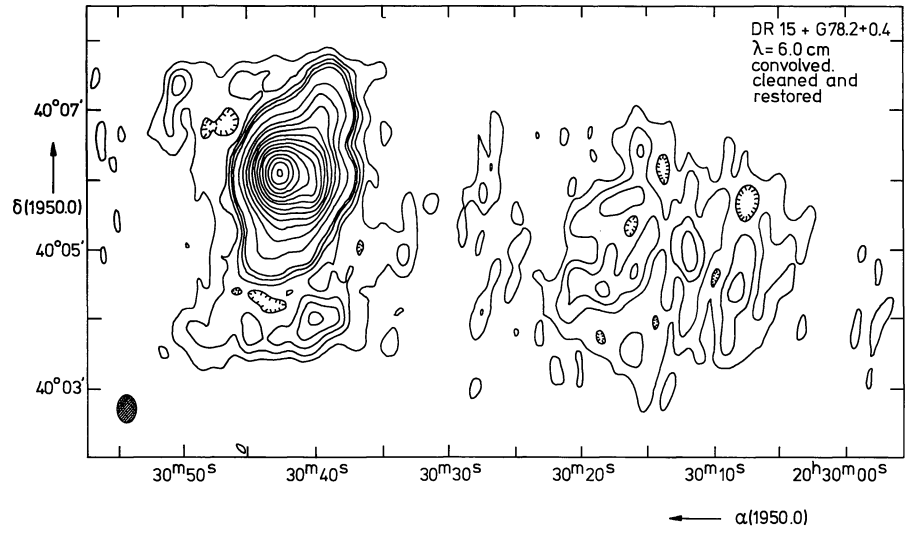

Fig. 10. DR 15 and G 79.2+1.0. Radio map at λ 6 cm convolved to a resolution of 15″. Contour values are 5, 10, 15, 20 and 25 m.f.u. per synthesized beam area, and then increase in steps of 25 to 375 m.f.u. per synthesized beam area

There are a few brightness maxima, the largest of which has dimensions of 1.5 (about 0.5 pc at 1 kpc distance) and a flux-density of about 100 m.f.u. This implies an r.m.s. electron-density of 95 cm^{-3} as compared to the average value of 57 cm^{-3}. The surface brightness of this maximum is only twice that of the surrounding medium.

The radio maxima visible in a map containing only spacings longer than 198 m, and thus insensitive to structure on a scale than 2′, all coincide with the optically brightest parts of S 125. The radio minima do not coincide exactly with the dark spots in front of the nebula, but are close to them. The excitation parameter derived from the radio observations is 16 pc cm^{-2}, which again fits a B0V – B0.5V star better than a BIV star (Panagia, 1973). Since the absolute magnitude of BD+46°3474 also favours a spectral type somewhat earlier than BIV, a small revision of the spectral type is suggested. S 125 is often regarded as a nebula whose exciting star is hidden (see for instance Morton, 1969). But since only a minor revision of the spectral type is needed, and since BD+46°3474 is very close to the center of the nebula (cf. Fig. 12), and also close to the brightest and presumably densest part of S 125, this conclusion seems unlikely.

In what stage of its evolution is S 125? Its low r.m.s. electron density, and the age of the associated cluster indicate that it is an old, fairly well-evolved HII region. No compact HII regions are found nearby; a few small-diameter sources north of S 125 (sources Nos. 24, 26 and 27 in Table 8; marked A, B and C in Fig. 12) are probably background objects, perhaps a multiple extragalactic radio source. The relatively small linear diameter (d=1.8 pc) of the nebula seems difficult to reconcile with a mass-limited model. Instead it seems likely that even at this stage S 125 is still photon-limited, mainly due to the presence of large amounts of high-density neutral matter and dust in its immediate vicinity. S 125 is associated with a large cloud of neutral hydrogen and carbon monoxide. Riegel (1967) found an HI cloud with a mass of 670 $M_\odot$ and typical dimensions of 10′ coinciding with S 125.

On the assumption that this cloud indeed is optically thin, and that it is spherical, a mean density n_{HI}=2100cm^{-3} is derived. The CO column densities are N_{CO}=1.0–1.6 10^{18} cm^{-2} (Milman et al., 1975). Taking a depth of 2.9 pc (corresponding to a size of 10′ for the cloud, one finds n_{CO}=0.1–0.2 cm^{-3}. Thus n_{CO}/n_{HI} appears to be 5– 10 10^{-5}, which seems to be a reasonable value. From these values, and from the relatively low r.m.s. electron-density of S 125, it seems clear that the ionized region must be located at the near edge of the neutral cloud. Tentatively one may conclude that at present star formation has stopped near S 125 although enough neutral matter still seems available.

8) S 142 (=NGC 7380, G107.2–1.0)

The red Palomar Sky Survey print shows S 142 as a nebula with a very complicated structure. The northern and southern edges have the fuzzy look of being mass-limited, while especially the eastern boundary is sharp and seems to be due to a cut-off by a large dust cloud complex. Near the eastern edge an irregular, thin dark lane crosses the nebula from north to south. From the western edge, a broad dark bay cuts into the nebula (Fig. 13).

The $8^m.6$ O6 star HD 215835, which is commonly thought to be the exciting star of S 142, is located rather excentrically in the nebula just north of this dark bay. The nebula S 142 contains most of the stars that belong to the OB association NGC 7380. This association was studied by Moffat (1971). He derived a distance of 3.6±0.7 kpc (slightly smaller than the dynamical value of 4.0 kpc used in this paper) and an age of 2 10^6 years

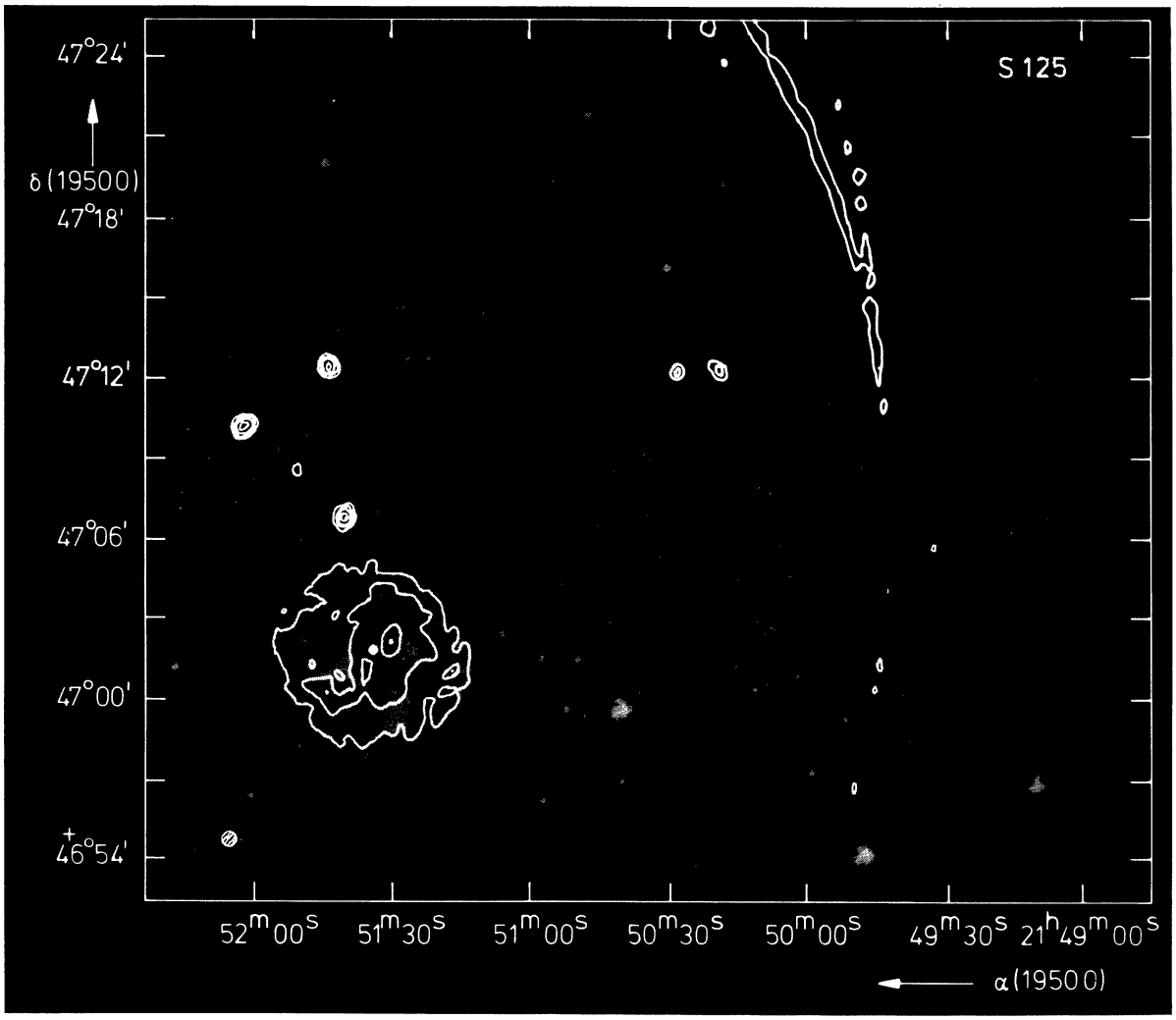

Fig. 11. S125. Radio contours at λ21 cm superimposed on the blue Palomar Sky Survey print. Contour values are 5, 8.75 and 15 m.f.u. per synthesized beam area

for the star cluster. The linear dimensions of the nebula (14×18 pc for $D=4$ kpc) imply a similar age.

The exciting star HD 215835 is a spectroscopical eclipsing binary also known as DH Cephei. Both components seem to be of the same spectral type O6. The double star has a colour excess $E(B-V)=0^{m}.66$. The reddening is normal (Johnson, 1966) so that about 2^{m} of visual extinction is implied.

In the eastern part of S 142 a more strongly reddened ($E(B-V)=0^{m}.81$) $10^{m}.6$ O9 star is present that may also contribute to the ionization of this part of the nebula, as may do an O5 star in the north.

The radio picture (Fig. 14) resembles the optical image. The low surface brightness radio structure of the nebula is rather symmetrical, while the contours of higher surface brightness have the shape of a letter "*V*". Remarkably little fine structure is visible in the radio-map, consistent with an advanced evolutionary stage in which most density-inhomogeneities have diffused into the surrounding medium. I marked the three OB stars mentioned before in Figure 14. In the λ 21 cm map, 12 flux-units are detected after correcting for primary beam effects, indicating that at least 65% of the total flux density of S 142 (see Table 4) has been observed, despite the size of the radio source relative to the shortest spacing of 170 wavelengths. The southwestern part of the nebula is probably most affected by missing-flux problems.

Since the derived physical parameters are not strongly dependent on the observed flux-density, the values in Table 9 will not be wrong by a large factor. The worst case will be the emission measure, which is linearly dependent on the flux-density.

The derived r.m.s. electron density of 25 cm^{-3} is what might be expected from an old HII region. The excitation parameter of 78 pc cm^{-2} indicates excitation by one O6 star. Two O6 stars and an O9 star can therefore be taken as amply sufficient for the ionization of

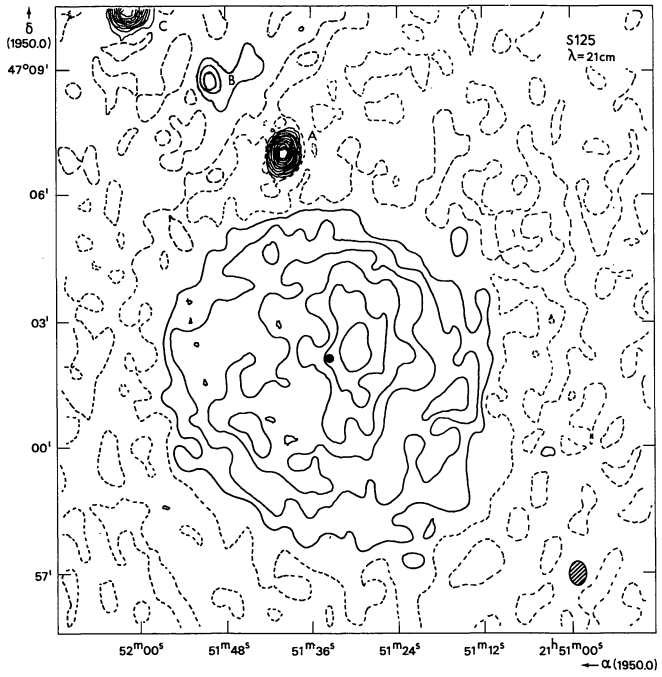

Fig. 12. S 125. Radio map at λ 21 cm showing contours of 2.5, 5, 7.5, 10, 12.5 and 15 m.f.u. per synthesized beam area. The zero contour is dashed. The sources marked A, B and C are listed as Nos. 24, 26 and 27 in Table 8. The central star BD+46°3474 is marked by a dot

S 142, even if it is largely mass-limited. Because the nebula seems to be well-evolved, the clumping factor is not likely to differ strongly from unity. This means that the ionized mass of S 142 indeed must be of the order of 2000 $M_\odot$. Thus the mass ratio of ionized gas versus exciting stars is here of the order of 25.

The only details that can be seen in the radiomap are a few condensations, most of which are in the eastern leg of the "V", and a few low brightness minima. Both the condensations and the minima have typical sizes comparable to the synthesized beamsize, i.e. linear sizes of about 0.5 pc. Near these condensations a small CO cloud ($d=5$ pc) is present at the same velocity as S 142 (Israël, unpublished). The minima coincide with the dark lanes; they do not reach the zerolevel. The maxima or condensations are located immediately adjacent to the dark lanes. This indicates that the dust lanes are not just in front of S 142, but that they are at least partially embedded in the nebula.

The condensations each have flux densities of about 10–30 m.f.u. Their total is only 200–300 m.f.u., i.e. only a few percent of the total flux density of S 142. Taking a mean diameter of 0.5 pc and a typical flux density value of 30 m.f.u., the r.m.s. electron density of a condensation is 135 cm^{-3}. This, together with the position of the condensations next to dark lanes makes it unlikely that they can be regarded as compact HII regions. Rather they are bright rims or externally ionized globules. This

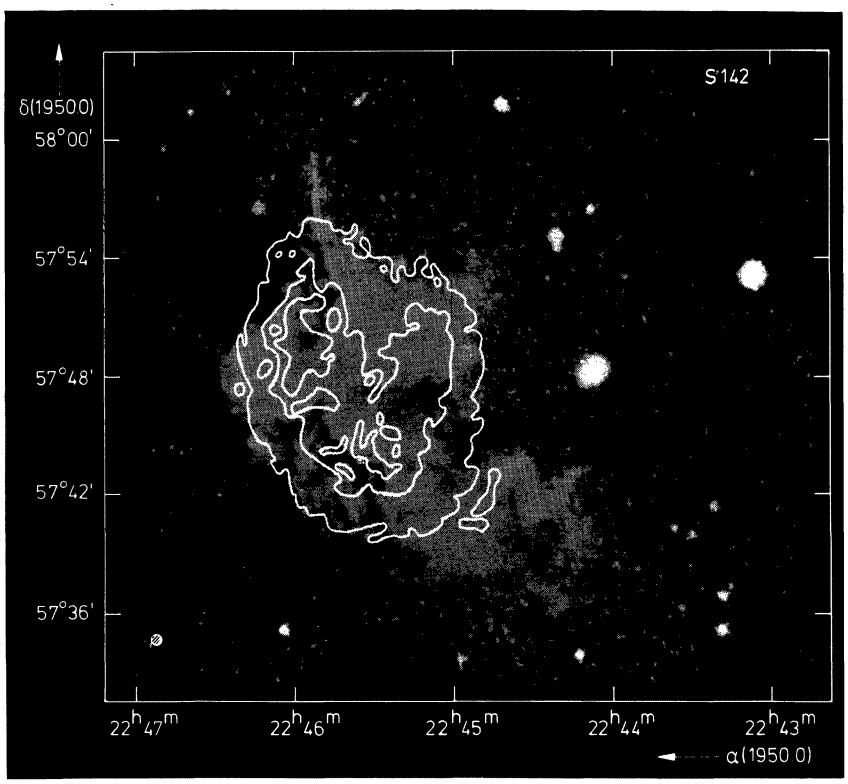

Fig. 13. S 142. Radio contours at λ 21 cm superimposed on the red Palomar Sky Survey print. Contour values are 5, 10 and 15 m.f.u. per synthesized beam area

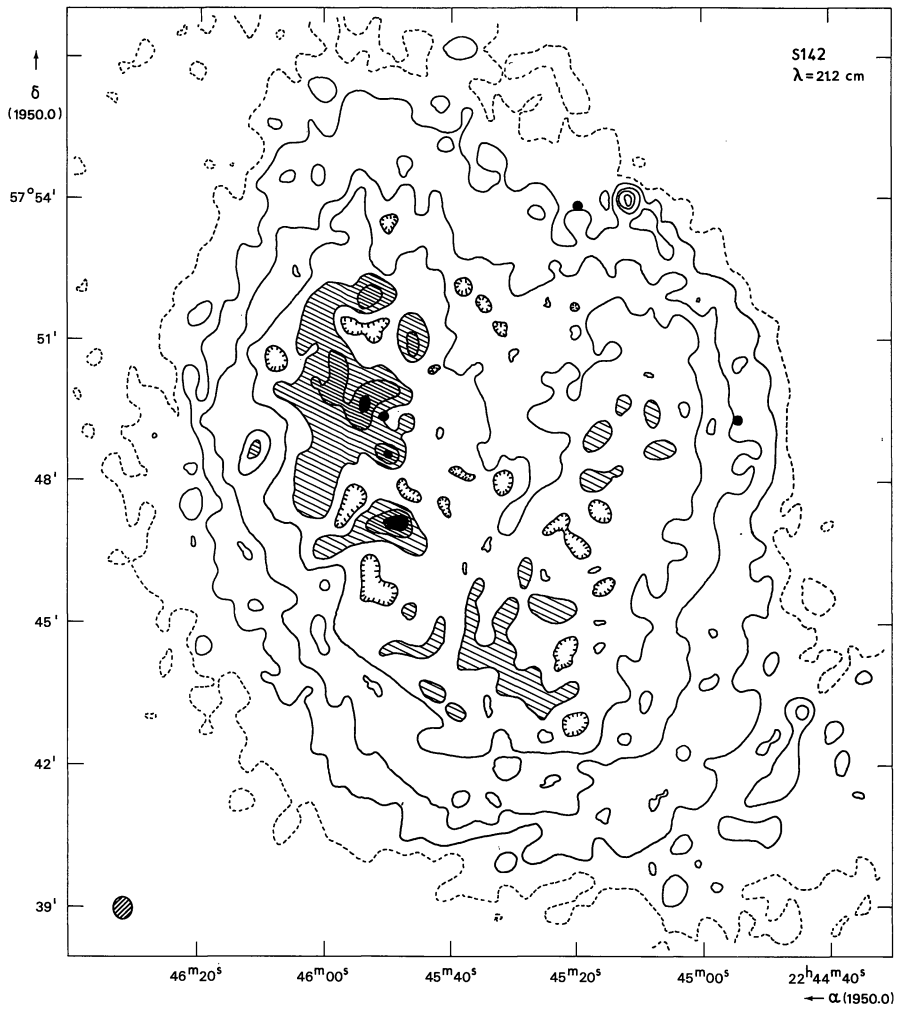

Fig. 14. S 142. Radio map at λ 21 cm showing contours of 5, 10, 15, 20, 25 and 30 m.f.u. per synthesized beam area. The zero contour is dashed. Dots mark the position of the stars (from left to right) LS II 57°90, LS II 57°83 and HD 215835. Small-scale structures are shaded.

fits in well with the notion of S 142 being an old HII region. Optical observations provide an easy check on this suggestion. If the condensations are merely the ionized edges of much denser neutral matter, their actual electron-densities will be much higher than the r.m.s. electron-density derived here, because of a geometry different from the homogeneous cylinder assumed in this present derivation. They also will show a relatively strong optical continuum. The condensations do not contrast strongly with the extended emission in the λ 21 cm map: the whole nebula has an emission measure of $0.7\ 10^4$ pc cm^{-6}, while the corresponding value for the condensations is $1.3\ 10^4$ pc cm^{-6}.

9) S 184 (NGC 281; G123.2−6.3)

S 184 is a relatively bright nebula on both the red and the blue Palomar Sky Survey prints (Fig. 15). Although its radiosize of 16′ (Caswell, 1968) is less than its optical size of 30′, it is still larger than the first grating ring in my λ 21 cm map, so that I could not observe the whole nebula. Indeed, in the map (Fig. 16) I detect only a total flux density of 6.2 f.u. out of 16 f.u. (cf. Table 4). The extended source has a size of only 7.2′. On the basis of the data in Tables 2 and 3, I adopt a distance $D=2$ kpc for S 184. This then leads to the rather low r.m.s. electron density $n_e=50\,\mathrm{cm}^{-3}$, and an excitation parameter $u=39$ pc cm^{-2}. Thus the part of the nebula represented in the map (which coincides with the optically brightest part of S 184, cf. Fig. 15) could be excited by only one O8 star. However, the exciting star of S 184 appears to be HD 5005, which has a spectral type of O5.5f (Georgelin, 1975). Such a star has an excitation parameter of 90 pc cm^{-2} (Panagia, 1973). Even when one takes the total flux density of 16 f.u., one derives only $u=57$ pc cm^{-2}, so that the nebula must be at least partially mass-limited (density-bounded). The position of HD 5005 and a nearby O9 star is indicated in Figure 16; note that both stars are located in a brightness minimum.

In the radio map, two regions of somewhat higher surface brightness are visible (designated A and B in Fig. 16). The overlay on the blue Palomar Sky Survey print (Fig. 15) shows them to be at the edge of the dark bay that cuts deeply into the nebula. The low surface brightness contours show that this dark bay is due to dust in front of the nebula, that is probably associated

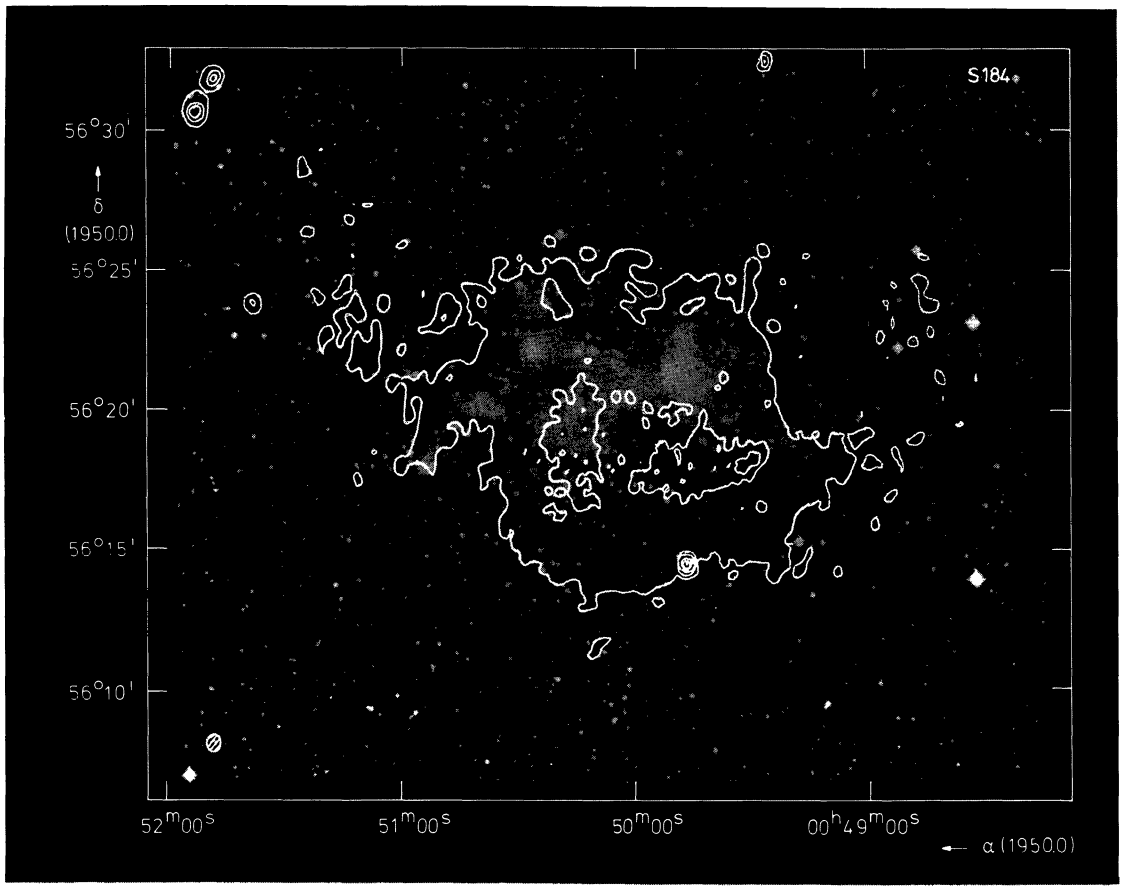

Fig. 15. S184. Radio contours at λ 21 cm are superimposed on the blue Palomar Sky Survey print. Contour values are 2.5, 15, 25, 50, 75 and 100 m.f.u. per synthesized beam area

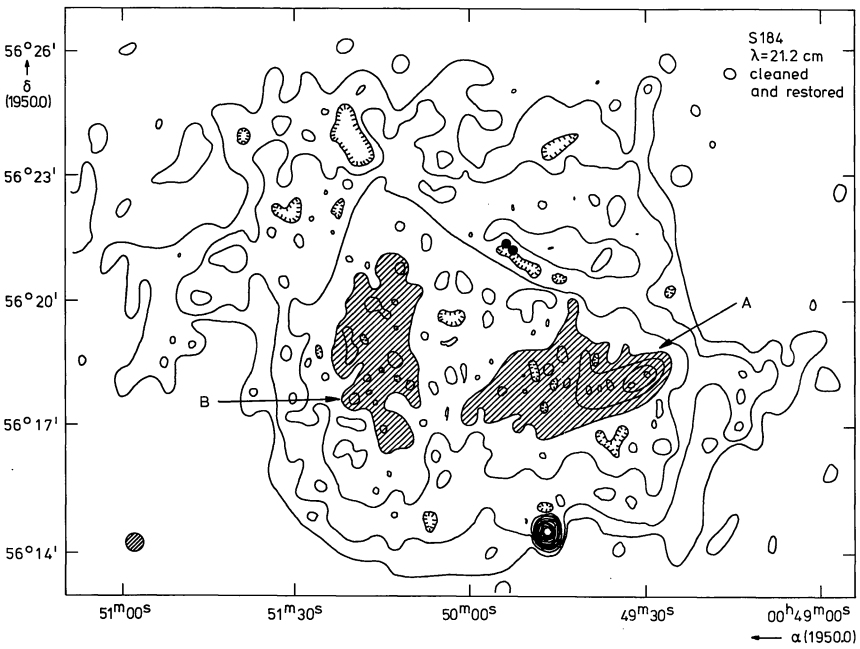

Fig. 16. S 184. Radio map at λ 21 cm, showing contours of 5, 10, 15, 20, 25, 30, 35, 40, 45, 50, 55, 60, 65, 70, 75, 80, 85, 90, 95 and 100 m.f.u. per synthesized beam area. Ridges *A* and *B* are shaded. The positions of the exciting star HD 5005 and a nearby early type star are marked by dots

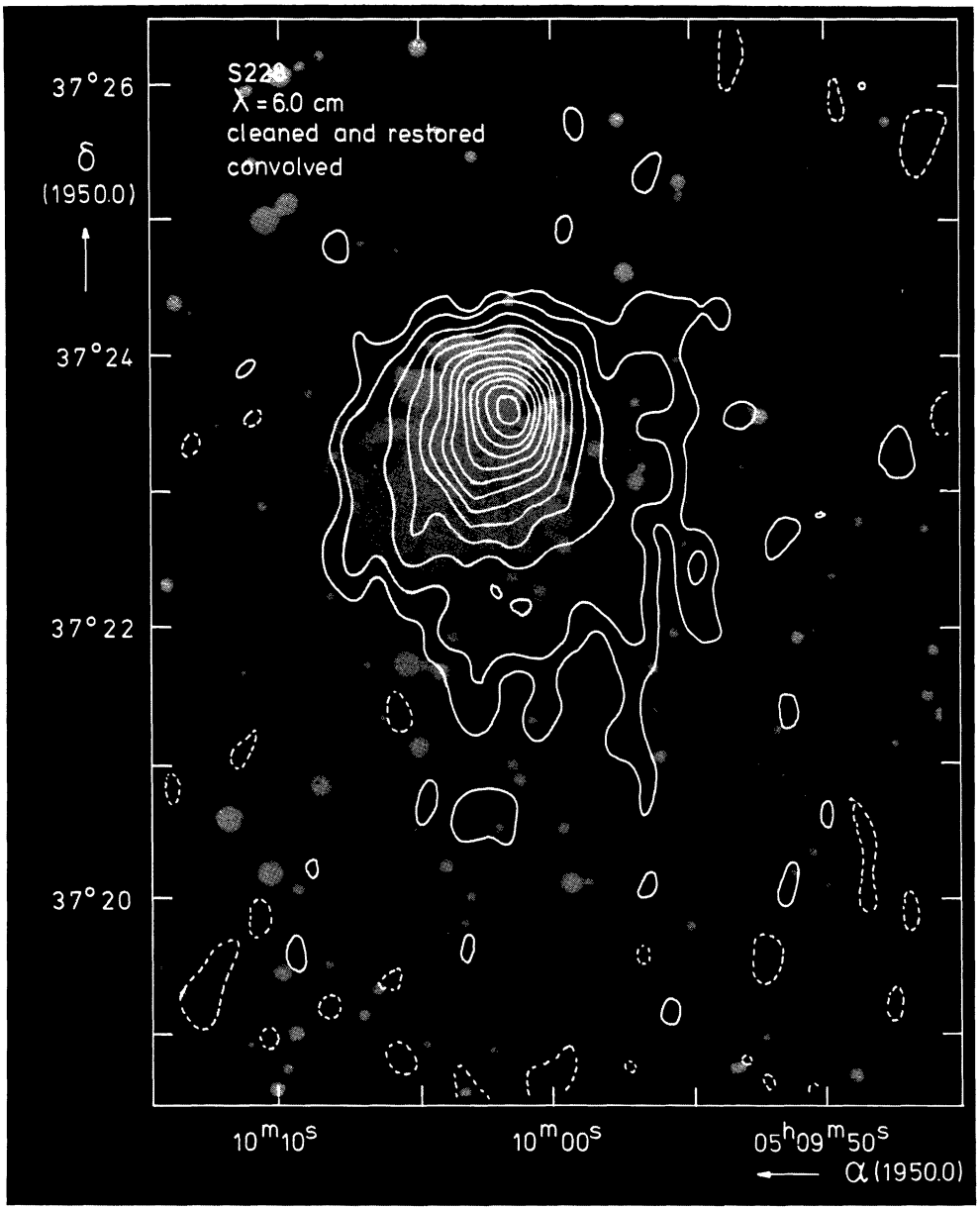

Fig. 17. S 228. Radio contours at λ 6 cm are superimposed on the red Palomar Sky Survey print. Contour values are 3, 6, 9, 12 and 15 m.f.u. per synthesized beam area. The radio map is convolved to a beam area of 15″

with it. The eastern edge of S 184 shows numerous bright rims/elephant trunks, that were studied by Pottasch (1956). Only at the position of his rims *D* and *E* some radio structure is visible. A weak radio peak (about 3 m.f.u.) coincides with the partially ionized globule *A*.

Riegel (1967) found a bright cloud of neutral hydrogen to be associated with S 184. Its center is somewhat to the southwest of S 184, and there is a minimum at the position of the nebula. The HI cloud has a size of about 50′, corresponding to about 35 pc at a distance of 2 kpc. Riegel (1967) estimated the mass of the cloud to be 16000 $M_\odot$, so that it will have a mean density $n_{HI}=30$ cm^{-3}. A large CO cloud ($d=15$ pc) is founds near S 184 (Israël, unpublished).

Thus this HII region appears to be old, at present ionized by a single star; a nebula moreover, in which most density inhomogeneities have already diffused into the surrounding medium.

10) A Small Source near S 184 (G123.11−6.36)

Of particular interest is the point source observed at the southern edge of S 184 (source No. 36 in Table 8). It is located in the middle of the dark bay and it is completely obscured. Although it might well be an extragalactic background source, its position at the edge of an extended HII region is highly suggestive of a connection with that region. Thus the source might be a compact HII region,

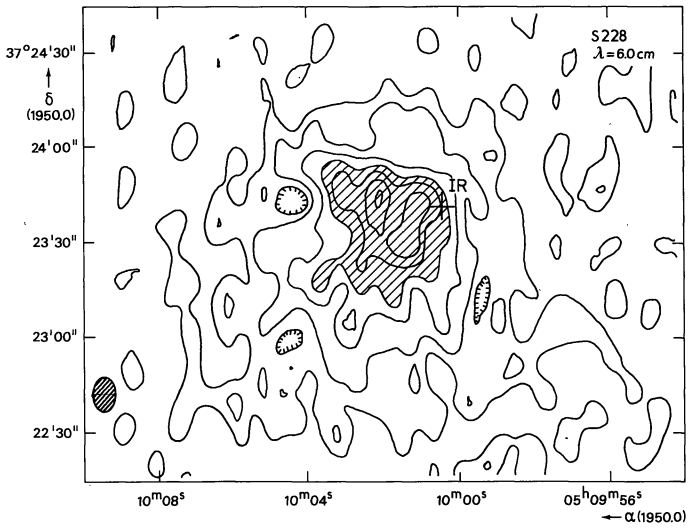

Fig. 18. S 228. Radio map at λ 6 cm, showing contours of 2, 4, 6, 8, 10, 12 and 14 m.f.u. per synthesized beam area. A cross marks the infrared position mentioned in the text

similar to S 158 G (Israël et al., 1973) or alternatively an obscured bright rim or ionized globule (cf. S 162 A, Israël et al., S 206 A, Deharveng et al., 1976). If it is associated with S 184, its parameters will be $n_e \geqslant 10^3$ cm^{-3}, $E.M. \geqslant 2\ 10^5$ pc cm^{-6} and $u \geqslant 10$ pc cm^{-2}.

11) S 228 (G169.19−0.90)

Optically, Sharpless 228 is a small symmetrical nebula about 2′ in diameter, located in a region which contains dust bands and diffuse emission regions (Fig. 17). It was observed mainly because an infrared source was found in it (Frogel and Persson, 1973). The infrared source consists of a hot, compact component (diameter less than 5″) surrounded by a less hot extended source (diameter over 55″).

The λ 6 cm radio observations (Fig. 18) give a different picture. They show appreciable structure in a core component, corresponding to Frogel and Persson's (1973) extended source. The core has a flux density $S_{4995} = 0.6$ f.u. and measures about 1′.5. It is surrounded by a radio envelope about twice as large, but with about the same radio flux density. Inside the core the infrared compact component (whose position is marked in Fig. 18) does not coincide with a radio feature.

On the basis of the Hβ emission observed by Frogel and Persson (1973) and their estimate of the extinction, one would expect a point source of at least 20 m.f.u. to be present in the map. Such a source would be clearly visible. The compact component can therefore not be compared to compact HII regions like K3-50 (Israël, 1976).

Rather the resemblance of the infrared source to the W3/IRS 5 source noted by Frogel and Persson is strengthened by the absence of radio emission. As they remark, the core of S 228 is hardly affected by extinction. From the λ 6 cm radio emission one expects $S_{2.2\,\mu m} = 0.2$ f.u. This is somewhat less than observed by Frogel and Persson in their 55″ diaphragm (although their result is uncertain due to the presence of the compact infrared source). Thus, not only at 3.5 μm, but even at 2.2 μm an infrared excess may be present. The total λ 6 cm flux-density of 1.3 f.u. is in good agreement with most single dish values tabulated in Table 4. Only the two points due to Churchwell and Walmsley (1973) are somewhat high. This, and the fact that Johnson (1974) observed only the core with a 2′.2 beam may indicate that the envelope extends beyond the 2′.9 diameter seen in my map. In the optical picture (Fig. 19) very weak diffuse emission on a scale of 4′.5 is visible. CO emission was detected in the direction of S 228 by Dickinson et al. (1974). The area was mapped in the CO line by Lucas and Encrenaz (1975). They found an extended cloud (10 × 6′) centered 5′ west of S 228 and a compact (2′) CO cloud or peak coinciding with the HII region.

The extended cloud has typical column densities $N_{CO} \approx 10^{18}$ cm^{-2} and a mass of 2000 $M_\odot$ while the small cloud has $N_{CO} = 10^{19}$ cm^{-2}. The compact CO cloud has a velocity $V_{LSR} = -5.3$ km s^{-1}, the extended cloud has velocities around $V_{LSR} = -10$ km s^{-1}. Because of its negligible extinction, S 228 must be in front of the CO cloud. The radial velocity of the ionized gas is $V_{LSR} = -9.4$ km s^{-1}. Thus S 228 appears to be expanding away from the CO cloud with a line of sight velocity component $V(\text{HII}-\text{CO}) = -4.1$ km s^{-1}. The presence of weak diffuse emission east of S 228 strengthens this conclusion considerably.

The presence of a point-like infrared source, possibly of the W3-IRS5 type, a dense CO cloud and radio continuum peaks with r.m.s. electron densities of the order of 1–2 10^3 cm^{-3} indicate that S 228 is a region in whose vicinity star formation is still going on, though probably on a modest scale.

References

Altenhoff, W.J., Downes, D., Goad, L., Maxwell, A., Rinehart, R.: 1970, *Astron. Astrophys. Suppl.* **1**, 319

Baars, J.W.M., Hooghoudt, B.G.: 1974, *Astron. Astrophys.* **31**, 323

Blair, G.N., Peters, W.L., Van den Bout, P.A.: 1975, *Astrophys. J. Letters* **200**, L161

Casse, J.L., Muller, C.A.: 1974, *Astron. Astrophys.* **31**, 333

Caswell, J.L.: 1968, Astron. J. **73**, 949

Chopinet, M., Lortet-Zuckermann, M.C.: 1975, *Astron. Astrophys.* (submitted)

Churchwell, E., Walmsley, C.M.: 1973, *Astron. Astrophys.* **23**, 117

Courtès, G., Cruvellier, P., Georgelin, Y.P., Astier, N.: 1966, *J. Obs.* **49**, 329

Davis, M.M.: 1967, *Bull. Astron. Inst. Neth.* **19**, 201

Deharveng, L., Israël, F.P., Maucherat, M.: 1976, *Astron. Astrophys.* **48**, 63

Dickel, J.R., Milne, D.K.: 1972, *Australian J. Phys.* **25**, 539

Dickinson, D.F., Frogel, J.A., Persson, S.E.: 1974, *Astrophys. J.* **192**, 347

Downes, D.: 1971, *Astron. J.* **76**, 305

Downes, D., Rinehart, R.: 1966, *Astrophys. J.* **144**, 937
Duin, R. M., Israël, F. P., Dickel, J. R., Seaquist, E. R.: 1975, *Astron. Astrophys.* **38**, 461
Emerson, J. P., Jennings, R. E., Moorwood, A. F. M.: 1973, *Nature Phys. Sci.* **241**, 109
Fanti, C., Felli, M., Ficarra, F., Salter, C. J., Tofani, G., Tomasi, P.: 1974, *Astron. Astrophys. Suppl.* **16**, 43
Felli, M., Curchwell, E.: 1972, *Astron. Astrophys. Suppl.* **5**, 369
Felli, M., Habing, H. J., Israël, F. P.: 1977, *Astron. Astrophys.* **59**, 43
Frogel, J. A., Persson, S. E.: 1973, *Astrophys. J.* 186, 207
Galt, J. A., Kennedy, J. E. D.: 1968, *Astron. J.* **73**, 135
Gebel, W. L.: 1968, *Astrophys. J.* **153**, 743
Georgelin, Y. M.: 1975, Thesis Univ. de Provence – Obs. de Marseille
Georgelin, Y. P., Georgelin, Y. M.: 1970, *Astron. Astrophys.* **6**, 349
Georgelin, Y. P., Georgelin, Y. M., Roux, S.: 1973, *Astron. Astrophys.* **25**, 337
Habing, H. J., Felli, M., Israel, F. P.: 1976 (in preparation)
Harris, S.: 1973, *Monthly Notices Roy. Astron. Soc.* **162**, 5P.
Harris, D. E., Roberts, J. A.: 1960, *Publ. Astron. Soc. Pacific* **72**, 237
Harten, R. H.: 1976, *Astron. Astrophys.* **46**, 109
Harten, R. H.: 1976 (in preparation)
Högbom, J.: 1974, *Astron. Astrophys. Suppl.* **15**, 417
Högbom, J., Brouw, W. N.: 1974, *Astron. Astrophys.* **33**, 289
Israël, F. P.: 1976, *Astron. Astrophys.* **48**, 193
Israël, F. P., Habing, H. J., de Jong, T.: 1973, *Astron. Astrophys.* **27**, 143
Johnson, H. L.: 1967, *Astrophys. J.* **147**, 912
Johnson, H. M.: 1974, in: HII Regions and the Galactic Center, 8th ESLAB Symposium, ed. A. F. M. Moorwood, ESRO SP105, p. 103
Johnson, H. M.: 1975, *Publ. Astron. Soc. Pacific* **87**, 89
Jong, T. de, Israël, F. P., Tielens, A. G. G. M.: 1975, in: HII Regions and Related Topics, eds. T. L. Wilson and D. Downes, Heidelberg, p. 123
Kazès, I., Le Squéren, A. M., Gadéa, F.: 1975, *Astron. Astrophys.* **42**, 9
Kellermann, K. I., Read, R. B.: 1965, *Publ. Owens Valley Radio Obs.* **1**, No. 2, p. 1
Lozinskaya, T. A., Esipov, V. F.: 1974, *Soviet Astron. A. J.* **17**, 449
Lucas, R., Encrenaz, P. J.: 1975, *Astron. Astrophys.* **41**, 233
Mezger, P. G., Henderson, A. P.: 1967, *Astrophys. J.* **147**, 741
Miller, J. S.: 1968, *Astrophys. J.* **151**, 473
Milman, A. S., Knapp, G. R., Knapp, S. K., Wilson, W. J.: 1975, *Astron. J.* **80**, 101
Milne, D. K.: 1970, *Australian J. Phys.* **23**, 425
Moffat, A. F. J.: 1971, *Astron. Astrophys.* **13**, 30
Morton, D. C.: 1969, *Astrophys. J.* **158**, 629
Osterbrock, D. E., Stockhausen, R. E.: 1961, *Astrophys. J.* **133**, 2
Panagia, N.: 1973, *Astron. J.* **78**, 929
Paschenko, V.: 1974, *Soviet Astron. A. J.* **17**, 438
Pottasch, S.: 1956, *Bull. Astron. Inst. Neth.* **13**, 77
RaghavaRao, R., Medd, W. J., Higgs, L. A., Broten, N. W.: 1965, *Monthly Notices Roy. Astron. Soc.* **129**, 159
Reifenstein, E. C., Wilson, T. L., Burke, B. F., Mezger, P. G., Altenhoff, W. J.: 1970, *Astron. Astrophys.* **4**, 357
Riegel, K. W.: 1967, *Astrophys. J.* **148**, 87
Shimmins, A. J., Day, G. A.: 1968, *Australian J. Phys.* **21**, 377
Someren Greve, H. W. van: 1974, *Astron. Astrophys. Suppl.* **15**, 343
Terzian, Y.: 1970, *Astron. J.* **75**, 1155
Terzian, Y., Pankonin, V.: 1972, *Astron. J.* **77**, 115
Walborn, N. R.: 1972, *Astron. J.* **77**, 312
Walker, M. F.: 1959, *Astrophys. J.* **130**, 57
Wendker, H. J.: 1968, *Astron. J.* **73**, 644
Wendker, H. J.: 1970, *Astron. Astrophys.* **4**, 378
Wendker, H. J.: 1971, *Astron. Astrophys.* **13**, 65
Whitford, A. E.: 1958, *Astron. J.* **63**, 201
Wilson, W. J., Schwartz, P. R., Epstein, E. E., Johnson, W. A., Etcheverry, R. D., Mori, T. T., Berry, G. G., Dyson, H. B.: 1974, *Astrophys. J.* **191**, 357